Protein Engineering, Design & Selection vol. 25 no. 6 pp. 307–311, 2012
Published online April 23, 2012 doi:10.1093/protein/gzs020

Engineered regulation of lysozyme by the SH3-CB1 binding interaction

Elizabeth Pham[1] and Kevin Truong[1,2,3]

[1]Institute of Biomaterials and Biomedical Engineering, University of Toronto, 164 College Street, Toronto, Ontario, Canada M5S 3G9 and [2]Edward S. Rogers Sr. Department of Electrical and Computer Engineering, University of Toronto, 10 King's College Circle, Toronto, Ontario, Canada M5S 3G4

[3]To whom correspondence should be addressed.
E-mail: kevin.truong@utoronto.ca

Received December 3, 2011; revised March 20, 2012; accepted March 26, 2012

Edited by David Ollis

The ability to design proteins with desired properties by using protein structural information will allow us to create high-value therapeutic and diagnostic products. Using the protein structures of lambda lysozyme and the SH3 domain of human Crk, we designed a synthetic protein switch that controls the activity of lysozyme by sterically hindering its active cleft through the binding of SH3 to its CB1 peptide-binding partner. First, several fusion protein designs with lysozyme and CB1 were modeled to determine the one with greatest steric effect in the presence of SH3. Next, the selected fusion protein was created and tested *in vitro*. In the absence of SH3, the lysozyme-CB1 fusion protein functioned normally. In the presence of SH3, the lysozyme activity was inhibited and with the addition of excess CB1 peptides to compete for SH3 binding, the lysozyme activity was restored. Lastly, this structure-based strategy can be used to engineer synthetic regulation by peptide-domain-binding interfaces into a variety of proteins.

Keywords: CB1 peptide/conformational space/protein switch/steric hindrance/SH3 domain

Introduction

Signaling pathways in cells are mediated and regulated by a wide host of modular domains. In particular, Crk adapter proteins consist almost entirely of Src homology 2 (SH2) and Src homology 3 (SH3) domains. SH2 domains bind to phosphorylated peptide sequences, while SH3 domains bind to short, linear, proline-rich sequences (Bar-Sagi *et al.*, 1993; Knudsen *et al.*, 1995). In humans, Crk proteins exist in two alternatively spliced forms, 28-kDa Crk1 and 42-kDa Crk2 (Buday, 1999). Although Crk2 contains two SH3 domains, only the 57-residue N-terminal SH3 domain (nSH3) has been shown to bind guanine nucleotide exchange factors including SOS and C3G (Feller *et al.*, 1994; Matsuda *et al.*, 1994; Ren *et al.*, 1994; Tanaka *et al.*, 1994). Knudsen *et al.* investigated the high-affinity binding of Crk2 and C3G. Their results revealed a Crk binding (CB1) peptide sequence of 10 amino acids (PPPALPPKKR) in C3G that showed both high affinity and specificity (K_d of 1.89 ± 0.06 μM) (Knudsen *et al.*, 1995). Finer molecular details regarding the interactions between SH3 domains and proline-rich motifs have been determined previously (Williamson, 1994; Wu *et al.*, 1995).

In addition to the important role enzymes play in signaling pathways, they cover a broad range of other catalytic activities. One such enzyme that is found in many different species is lysozyme, which is involved in the digestion of bacterial cell walls. Bacterial viruses like bacteriophage lambda use lysozyme as part of the infection cycle, to release their newly synthesized virions. Crystal structure studies of lambda lysozyme complexed with oligosaccharides (Duewel *et al.*, 1995; Leung *et al.*, 2001) revealed several key structural features and molecular interactions between lysozyme and its substrates. Lambda lysozyme is a small 158-residue globular protein with approximate dimensions of 40 Å × 32 Å × 32 Å (Evrard *et al.*, 1998). It is divided equally into a lower and an upper domain connected by an α-helix. While the upper domain consists mainly of α-helices, the lower domain is composed mainly of β-sheets. Between these domains, a deep elongated active site cleft is formed (Leung *et al.*, 2001). The crystal structure of lambda lysozyme has also revealed two different conformations of the protein where the active site appears in either an open or a closed conformation. Evrard *et al.* provided mechanistic evidence for the need of a large conformational change for the function of lambda lysozyme (Evrard *et al.*, 1999). Interestingly, the conformational change is not due to a hinge-bending motion between the lower and upper domains, but is a consequence of a peptide segment in the upper domain moving toward the active site in the presence of a bound oligosaccharide substrate. This peptide segment is pulled back, fully opening the active site when the enzyme is unoccupied (Evrard *et al.*, 1999; Leung *et al.*, 2001).

While other groups have used modular domains to engineer synthetic proteins for rewiring signaling pathways (Dueber *et al.*, 2004), these proteins were not engineered by modeling changes in the protein conformational space which could have helped improve designs. Previously, our group developed a computational tool called FPMOD that generates the conformational space of protein-based Ca^{2+} biosensors to estimate changes in fluorescence signal upon binding to Ca^{2+} (Pham *et al.*, 2007). Other groups have also used this tool to estimate changes in separation distances between ligand-bound and -unbound growth factor receptors (Kozer *et al.*, 2010) or sarcoendoplasmic reticulum Ca^{2+}-ATPase (Winters *et al.*, 2008). Conceivably, the analysis of the protein conformational space could also be used to estimate steric hinderance of the enzymatic active sites. To demonstrate this utility, we designed a synthetic fusion protein to regulate the transglycosylase activity of lambda lysozyme by means of the SH3-CB1 binding interaction. First, conformational space analysis on lysozyme-CB1 fusion proteins revealed the candidate with the best potential to inhibit lysozyme activity upon binding to nSH3. Then, experimental

in vitro studies showed this synthetic fusion protein retained lysozyme activity that could be inhibited by nSH3 and restored by competitively inhibiting nSH3 with CB1 peptides. Thus, nSH3 domain and CB1 peptide could serve as inputs to turn the function of lysozyme on and off. This study sheds light on how Nature uses modular domains to engineer regulation into a variety of proteins and further, this structure-based strategy can be applied to other enzymes to introduce synthetic regulation by modular domains.

Materials and methods

Plasmids

All fragments used were inserted to pCfVtx3 (Truong *et al.*, 2003) after polymerase chain reaction from plasmid or cDNA sources. Lysozyme was amplified from bacteriophage lambda cDNA; nSH3 was amplified from the PicchuX plasmid given by Matsuda M. (Kyoto University); CB1 was created by overlapping primers. Then, the fusion proteins Venus-CB1-Lysozyme (VCL), Venus-CB1-Lysozyme-CB1 (VCLC), Venus-CB1 and His-nSH3C were assembled by our previously described cassette-based methodology (Truong *et al.*, 2003; Pham and Truong, 2010).

Protein expression

Escherichia coli DH5-α cells were transformed with the respective plasmids. Cells were grown overnight and leak expression was used to accumulate proteins. The cells were sonicated using a Branson Sonifier 250 at a setting of 20% duty cycle and 2.5 output control for 0.5–1.5 min. Final protein concentrations were determined by fluorescence intensity compared with standard solutions where the fluorescent protein concentration was previously measured by a Bradford assay. Fluorescence was imaged with the IllumaTool portable lighting system (Light Tools Research, Pasadena, CA, USA). Cerulean was excited and observed with a 440 ± 10 nm bandpass filter and 475 nm longpass filter, respectively; Venus was excited and observed with a 488 ± 20 nm bandpass filter and 525 nm longpass filter, respectively; monomeric red fluorescent protein (mRFP) was excited and observed with a 540 ± 20 nm bandpass filter and 580 nm longpass filter, respectively.

Pulldown assay

A solution of His-nSH3C protein was mixed with Ni^{2+}–NTA agarose beads (Qiagen) and incubated at room temperature for 30 min. Unbound His-nSH3C was rinsed away twice with a wash buffer solution (25 mM Tris, 50 mM NaCl, pH 8). A solution of VCLC protein was mixed with the His-nSH3C-immobilized beads and incubated another 30 min at room temperature. Again, unbound VCLC was rinsed away twice with a wash buffer solution (25 mM Tris, 50 mM NaCl, pH 8). Beads (20 μl) were loaded on a sodium dodecyl sulfate polyacrylamide gel electrophoresis (SDS-PAGE). The SDS-PAGE was done using the NuPAGE system (4–12% Bis-Tris gels) according to the manufacturer's instructions (Invitrogen). For fluorescence screening, IllumaTool portable lighting system was used (Light Tools Research, Pasadena, CA, USA).

Cell lysing assay

Escherichia coli DH5-α cells were transformed with plasmids expressing mRFP (Campbell *et al.*, 2002). Cells alone or with protein solutions were placed into a −70°C freezer. After the solutions were frozen, they were thawed at room temperature. Solutions were spun down and 20 μl of the supernatant was loaded on an SDS-PAGE.

Results and discussion

Conceptual design of lysozyme fusion proteins

In theory, the steric hindrance of lysozyme can be modulated by the binding of SH3 to CB1 peptides engineered into lysozyme (Fig. 1). Steric hindrance of lysozyme might inhibit a substrate from binding the active cleft resulting in reduced transglycosylase activity. Structurally, the active site of lysozyme is a cleft running across the middle of the protein, flanked top and bottom by two halves of the protein. For lysozyme to function as a transglycosylase, its active cleft lines up with an oligosaccharide strand of the bacterial peptidoglycan layer. Due to the proximity of the N- and C-termini of lysozyme to the active cleft, the fusion of the CB1 peptide to either or both termini would allow intermolecular SH3 binding that may sterically hinder the active cleft. To verify this hypothesis, we studied the conformational space of the fusion proteins Venus-Lysozyme-CB1 (VLC), VCL and VCLC in the absence or presence of nSH3-Cerulean (nSH3C) using models created by our

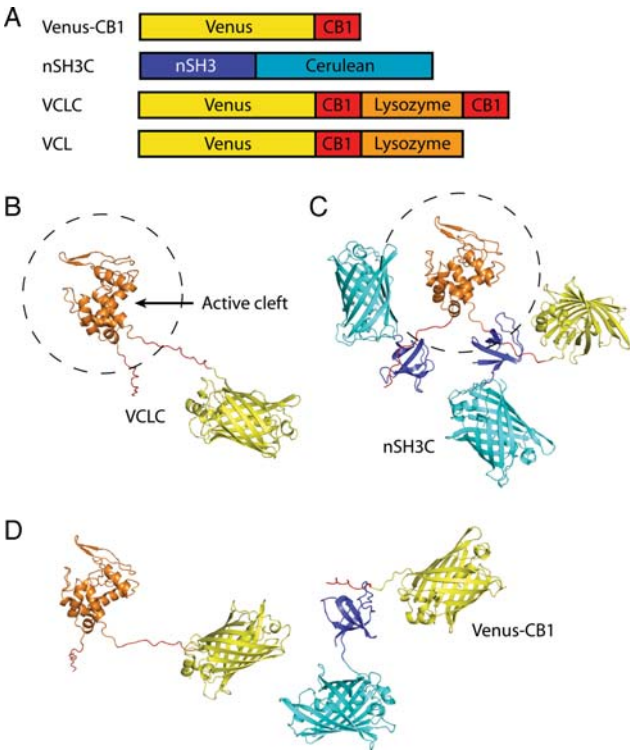

Fig. 1. Protein models. (**A**) Schematic layout of engineered fusion proteins—Venus-CB1, nSH3C, VCL and VCLC. Structural models for (**B**) VCLC alone (i.e. lysozyme is active), (**C**) VCLC bound with nSH3C (i.e. lysozyme is inactive) and (**D**) VCLC with Venus-CB1 competitively bound to nSH3C (i.e. lysozyme is active). Venus is colored yellow; CB1, red; nSH3, blue; Cerulean, cyan; lysozyme, orange. Dashed lines indicate defined spherical volume around lysozyme.

Table I. Conformational space analysis of steric hindrance on lysozyme active cleft.

Construct	No. of atoms in defined volume[a]	Percentage change in steric hindrance[b]
VLC unbound	1073	67%
VLC bound	1797	
VCL unbound	668	53%
VCL bound	1025	
VCLC unbound	643	83%
VCLC bound	1176	

Average percentage change in the degree of steric hindrance on each construct modeled between the nSH3C unbound and bound cases. Reported are percentage changes for a sphere of radius 50 Å.
[a]Number of atoms within the defined volume only include atoms that were not from the lysozyme protein itself.
[b]Averaged for $n = 500$ models. Percentage change = No. of atoms bound minus unbound/no. of atoms unbound.

computational tool—FPMOD (Pham *et al.*, 2007). Venus (Nagai *et al.*, 2002) and Cerulean (Rizzo *et al.*, 2004) are yellow fluorescent protein and cyan fluorescent protein variants, respectively, with improved brightness to allow quantification by fluorescence.

VCLC fusion protein had the largest computed steric effects

From three different lysozyme-CB1 fusion proteins modeled (i.e. VLC, VCL and VCLC), VCLC had the greatest steric effects in the presence of the fusion protein nSH3C (Fig. 1) (Table I). FPMOD (Pham *et al.*, 2007) was used to generate models ($n = 500$) for VLC, VCL and VCLC bound and unbound to nSH3C that formed the protein conformational space. To assess the steric hindrance of the active cleft, a spherical region was defined around the lysozyme protein in each fusion construct. The change in steric hindrance was defined as the percentage change in the number of atoms within the defined region between the nSH3C unbound and bound cases. The center of the sphere was chosen to be a carbon alpha atom of residue Tyr 67 which spatially corresponds to the center of lysozyme. The distance between the center atom and the furthest atom is approximately 25 Å. From this chosen center, spheres of radii 25, 50 and 100 Å were defined. It was determined that at radius 25 Å, only atoms belonging to the lysozyme protein were enclosed in all constructs modeled. Also, at 100 Å, all atoms were enclosed within the bounded volume. We thus compared the number of atoms (minus those of lysozyme) enclosed within a sphere of radii of 50 Å (Table I). It is noteworthy that placing lysozyme right after the Venus in VLC had greater steric hindrance (i.e. number of atoms in the defined region) in both the unbound and bound cases than for VCL. We speculate that this is due to the proximity of Venus interfering with the active cleft of lysozyme. Nonetheless, we found that VCLC had the greatest change in steric hindrance in the presence of bound nSH3C. Thus, VCLC was chosen for further *in vitro* tests.

VCLC binds nSH3C in vitro

The binding of VCLC to nSH3C was confirmed using a Ni^{2+}–NTA pulldown assay (Fig. 2). The fusion protein VCLC was created as a tandem fusion of Venus (Nagai *et al.*, 2002), the CB1 peptide, lysozyme and the CB1 peptide, while His-nSH3C was a tandem fusion of a polyhistidine tag, nSH3 and Cerulean (Rizzo *et al.*, 2004). His-nSH3C was recruited to Ni^{2+}–NTA beads through binding of the polyhistidine tag. After washing the beads of unbound His-nSH3C, various concentrations of VCLC were added to the Ni^{2+}–NTA beads loaded with His-nSH3C. After washing the beads of unbound VCLC, the Ni^{2+}–NTA beads were loaded on SDS-PAGE where VCLC should run at the size of 42 kDa and His-nSH3C, at 35 kDa. Due to the viability of the fluorescent protein's chromophore, the fluorescence was still detectable on the gel despite treatment with SDS. At low concentrations (i.e. 0.1 μM) of VCLC, His-nSH3C was unable to recruit the protein, but at higher concentrations (i.e. 0.5, 1, 2 μM), the recruitment was evident (Fig. 2A). Even before loading on the SDS-PAGE, the recruitment of His-nSH3C to the Ni^{2+}–NTA beads and subsequent recruitment of VCLC was noticeable in Eppendorf tubes (Fig. 2B).

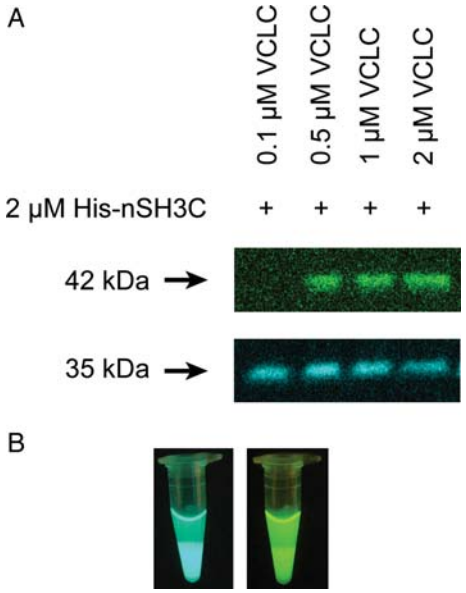

Fig. 2. Pulldown assay for the binding of VCLC to His-nSH3C. (**A**) Fluorescence SDS-PAGE of mixtures of His-nSH3C and VCLC. After immobilized to Ni^{2+}–NTA beads via its polyhistidine tag, His-nSH3C was subsequently used to recruit VCLC. Note that VCLC runs at the size of 42 kDa while His-nSH3C, at 35 kDa. (**B**) Eppendorf tubes with a mixture of His-nSH3C immobilized beads and VCLC. The Cerulean (left) and Venus fluorescence channels (right) of the same Eppendorf tube showed co-localization, indicating binding of VCLC to His-nSH3C. The concentration for nSH3C and VCLC is 2 μM.

VCLC retains lysozyme activity

Despite its fusion with CB1 peptides, VCLC retains lysozyme's function to lyse cells (Fig. 3). Lambda lysozyme lyses bacterial cell walls by cleaving the peptidoglycan layers in a process that releases their cytoplasmic contents into the growth media. To make the release of cell contents detectable, we lysed *E.coli* cells transformed with mRFP (Campbell *et al.*, 2002) (Fig. 3A). Since *E.coli* cells have an extra outer membrane protecting its peptidoglycan layer, it was necessary to assist the activity of lysozyme by freeze–thawing the cells. In particular, the cell solutions were placed into a −70°C freezer to slowly freeze and form water crystals that caused small breaks in the outer membrane.

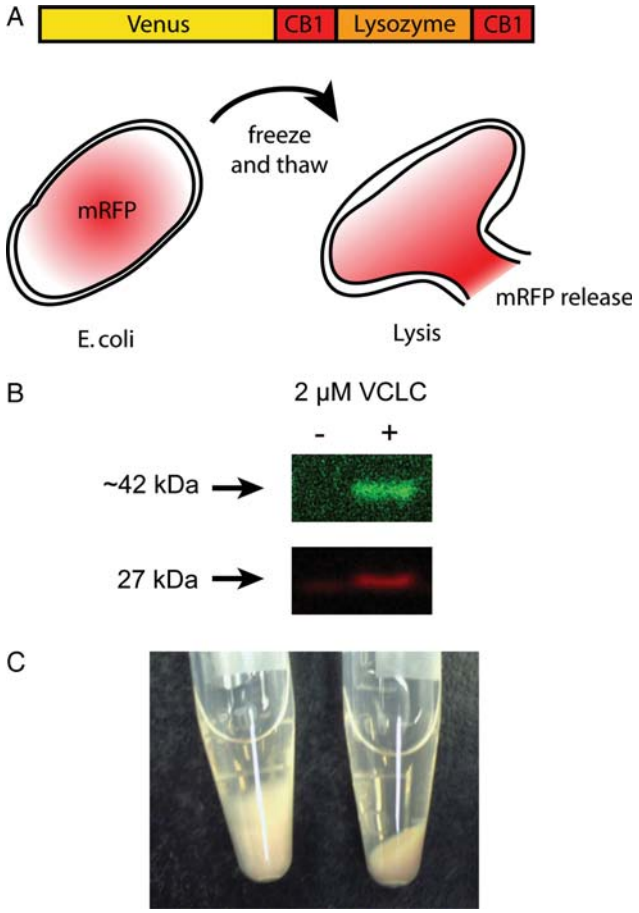

Fig. 3. Cell lysis assay for detecting the lysozyme activity of VCLC. (**A**) A cartoon depicting the cell lysis assay. After cells transformed with mRFP are lysed with VCLC, mRFP leaks into the growth media. Freeze–thawing helps enhance the action of lysozyme by allowing easier access to the peptidoglycan layer encased by the outer membrane of the *E.coli* cell. (**B**) Fluorescence SDS-PAGE of growth media of cells alone or mixed with VCLC. The detection of red fluorescence indicated cell lysis. Note that VCLC runs at the size of 42 kDa while mRFP, at 27 kDa. (**C**) Eppendorfs with cells mixed with VCLC (left) or cells alone (right) showed cell debris as a soft mass.

Then, the frozen solution was thawed slowly at room temperature. As the solution thawed, lysozyme was able to diffuse through the breaks in the outer membrane to reach the peptidoglycan layer. Using this approach, cell lysis solutions were loaded on SDS-PAGE and compared between cells alone and cells mixed with 2 μM VCLC for the appearance of released mRFP running at the size of 27 kDa. While there was some mRFP detected in the case of cells alone (indicating that the freeze–thaw procedure has some intrinsic ability to lyse cells), there was significantly more mRFP release in the case of VCLC (Fig. 3B). Even before loading on the SDS-PAGE, the cell lysis with VCLC was noticeable in Eppendorf tubes as a soft mass of cell debris (Fig. 3C).

VCLC is inhibited by His-nSH3C and restored by competitive Venus-CB1

In vitro cell lysis assays showed that the lysozyme activity of VCLC was reduced in the presence of His-nSH3C and was partially restored by competitive inhibition with Venus-CB1 (Fig. 4). Using the above cell lysis assay, the ability of VCLC to lyse cells was assessed with varying concentrations

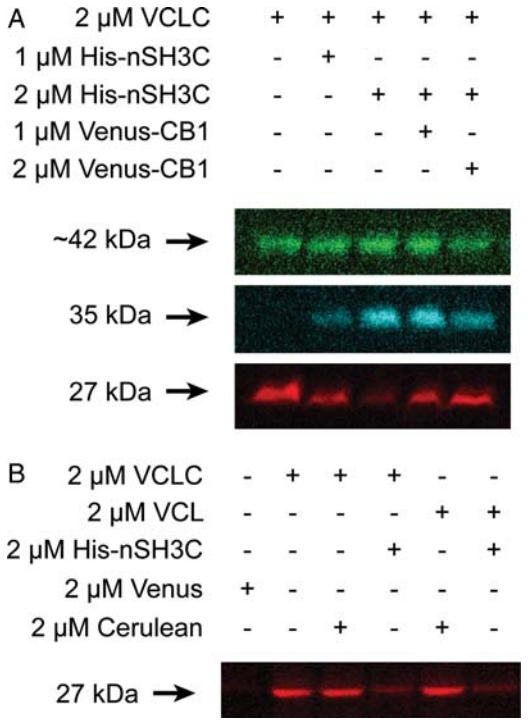

Fig. 4. (**A**) Fluorescence SDS-PAGE of growth media of cells with mixtures of VCLC, His-nSH3C and Venus-CB1. Under a constant concentration of VCLC, increasing concentrations of His-nSH3C caused reduced cell lysis. Under a constant concentration of both VCLC and His-nSH3C, increasing concentrations of competing Venus-CB1 caused increased cell lysis. (**B**) Fluorescence SDS-PAGE of growth media of cells with mixtures of VCLC, VCL, His-nSH3C, Venus and Cerulean. Note that VCLC runs at the size of 42 kDa; His-nSH3C, at 35 kDa; mRFP, at 27 kDa. Venus-CB1 also runs at the size of 27 kDa, but was not visible due to the strong mRFP band.

of His-nSH3C and Venus-CB1 (Fig. 4A). First, VCLC was kept constant at 2 μM. With only VCLC, the cells were similarly lysed as before as indicated by the release of mRFP. As His-nSH3C was increased from 1 to 2 μM, VCLC was more inhibited as decreasing mRFP was released. Thus, His-nSH3C inhibits the activity of VCLC. Next, both VCLC and His-nSH3C were kept constant at 2 μM. As Venus-CB1 was increased from 1 to 2 μM, VCLC was less inhibited as increasing mRFP was released. Thus, Venus-CB1 competed with VCLC for His-nSH3C binding, thereby allowing free VCLC to lyse cells. Together, these proteins form a network where VCLC activity is controlled by His-nSH3C and Venus-CB1. As control, we showed that VCLC inhibition was dependent on the SH3-CB1 binding interaction since mixture with Cerulean had no effect on lysozyme activity (Fig. 4B). Furthermore, we showed VCL was similarly inhibited by His-nSH3C, suggesting that one CB1 site is sufficient for inhibition (Fig. 4B).

Conclusions

From structural information available, we designed a synthetic fusion protein to regulate the lysozyme activity by the SH3-CB1 binding interaction. This synthetic fusion protein retained lysozyme activity that could be inhibited by nSH3 and restored by competitively inhibiting nSH3 with CB1 peptides. Thus, one way in which modular domains can

regulate biological functions in Nature is by sterically hindering the target protein. This knowledge combined with a structure-based strategy can be used to engineer regulation into a variety of proteins by modular domains. Further, by adding other control mechanisms such as Ca^{2+} signaling (Mills *et al.*, 2010; Mills and Truong, 2010) and photoactivation (Pham *et al.*, 2011), we can engineer more complex protein regulatory networks.

Funding

This work was supported by grants from the Canadian Institutes of Health Research (#81262) and the National Science and Engineering Research Council (#283170).

References

Bar-Sagi,D., Rotin,D., Batzer,A., Mandiyan,V. and Schlessinger,J. (1993) *Cell*, **74**, 83–91.
Buday,L. (1999) *Biochim. Biophys. Acta*, **1422**, 187–204.
Campbell,R.E., Tour,O., Palmer,A.E., Steinbach,P.A., Baird,G.S., Zacharias,D.A. and Tsien,R.Y. (2002) *Proc. Natl Acad. Sci. USA*, **99**, 7877–7882.
Dueber,J.E., Yeh,B.J., Bhattacharyya,R.P. and Lim,W.A. (2004) *Curr. Opin. Struct. Biol*, **14**, 690–699. First published on 8 December 2004.
Duewel,H.S., Daub,E. and Honek,J.F. (1995) *Biochim. Biophys. Acta*, **1247**, 149–158.
Evrard,C., Fastrez,J. and Declercq,J.P. (1998) *J. Mol. Biol.*, **276**, 151–164.
Evrard,C., Fastrez,J. and Soumillion,P. (1999) *FEBS Lett.*, **460**, 442–446.
Feller,S.M., Knudsen,B. and Hanafusa,H. (1994) *EMBO J.*, **13**, 2341–2351.
Knudsen,B.S., Zheng,J., Feller,S.M., Mayer,J.P., Burrell,S.K., Cowburn,D. and Hanafusa,H. (1995) *EMBO J.*, **14**, 2191–2198.
Kozer,N., Henderson,C., Bailey,M.F., Rothacker,J., Nice,E.C., Burgess,A.W. and Clayton,A.H. (2010) *Biochemistry*, **49**, 7459–7466. First published on 19 August 2010.
Leung,A.K., Duewel,H.S., Honek,J.F. and Berghuis,A.M. (2001) *Biochemistry*, **40**, 5665–5673.
Matsuda,M., Hashimoto,Y., Muroya,K., Hasegawa,H., Kurata,T., Tanaka,S., Nakamura,S. and Hattori,S. (1994) *Mol. Cell. Biol.*, **14**, 5495–5500.
Mills,E., Pham,E. and Truong,K. (2010) *Cell Calcium*, **48**, 195–201.
Mills,E. and Truong,K. (2010) *Cell Calcium*, **47**, 369–377.
Nagai,T., Ibata,K., Park,E.S., Kubota,M., Mikoshiba,K. and Miyawaki,A. (2002) *Nat. Biotechno.l*, **20**, 87–90.
Pham,E., Chiang,J., Li,I., Shum,W. and Truong,K. (2007) *Structure*, **15**, 515–523.
Pham,E., Mills,E. and Truong,K. (2011) *Chem. Biol.*, **18**, 880–890.
Pham,E. and Truong,K. (2010) *Methods Mol. Biol.*, **591**, 69–91.
Ren,R., Ye,Z.S. and Baltimore,D. (1994) *Genes Dev.*, **8**, 783–795.
Rizzo,M.A., Springer,G.H., Granada,B. and Piston,D.W. (2004) *Nat. Biotechnol.*, **22**, 445–449.
Tanaka,S., Morishita,T., Hashimoto,Y., *et al.* (1994) *Proc. Natl Acad. Sci. USA*, **91**, 3443–3447.
Truong,K., Khorchid,A. and Ikura,M. (2003) *BMC Biotechnol.*, **3**, 8.
Williamson,M.P. (1994) *Biochem. J.*, **297**(Pt 2), 249–260.
Winters,D.L., Autry,J.M., Svensson,B. and Thomas,D.D. (2008) *Biochemistry*, **47**, 4246–4256.
Wu,X., Knudsen,B., Feller,S.M., Zheng,J., Sali,A., Cowburn,D., Hanafusa,H. and Kuriyan,J. (1995) *Structure*, **3**, 215–226.